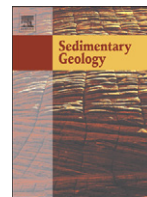




Contents lists available at SciVerse ScienceDirect

## Sedimentary Geology

journal homepage: [www.elsevier.com/locate/sedgeo](http://www.elsevier.com/locate/sedgeo)

## Detrital supply from subduction/accretion complexes to the Eocene–Oligocene post-collisional southern Thrace Basin (NW Turkey and NE Greece)

Azzurra d'Atri <sup>a</sup>, Gian Gaspare Zuffa <sup>a</sup>, William Cavazza <sup>a,\*</sup>, Aral I. Okay <sup>b</sup>, Gianfranco Di Vincenzo <sup>c</sup>

<sup>a</sup> Dipartimento di Scienze della Terra e Geologico-ambientali, Università di Bologna, Italy

<sup>b</sup> Avrasya Yerbilimleri Enstitüsü ve Jeoloji Mühendisliği Bölümü, Maden Fakültesi, İstanbul Teknik Üniversitesi, Maslak, İstanbul, Turkey

<sup>c</sup> Istituto di Geoscienze e Georisorse, Consiglio Nazionale delle Ricerche, Pisa, Italy

## ARTICLE INFO

## Article history:

Received 23 December 2010

Received in revised form 1 October 2011

Accepted 14 October 2011

Available online 20 October 2011

Editor: G.J. Weltje

## Keywords:

Sandstone petrology

Heavy minerals

Turbidites

Sediment paleodispersal system

## ABSTRACT

The Thrace Basin is a large, mostly Eocene–Oligocene post-collisional sedimentary basin which developed following the closure of the Vardar–İzmir–Ankara oceanic domain (latest Cretaceous–Paleocene). Sandstone petrologic data (framework and heavy-mineral analyses) and the synthesis of preexisting and new sedimentological observations along representative stratigraphic sections show that the basin fill of the southern Thrace Basin was mostly derived from the İzmir–Ankara and Biga (?Intra-Pontide) subduction/accretion complexes to the south. Proximal facies consistently show northward paleocurrents whereas most paleocurrent indicators measured downcurrent point to an eastward paleoflow, likely the result of the deflection of primary gravity flows originated along the southern margin of the basin. Detrital contributions from the Rhodopian basement complex to the west are virtually absent within the southern Thrace Basin fill. Conversely, Rhodopes-derived, Eocene proximal facies in northeastern Greece are characterized by a series of coarse-grained fan-deltas prograding eastward and likely feeding the basin–plain turbidites of the depocentral portion of the Thrace basin, now concealed in the subsurface to the north of our study area.

Arenites of the southern Thrace Basin are mostly lithic arkoses and arkosic litharenites. Provenance from the İzmir–Ankara and Biga suture zones to the south is characterized by ophiolitic, granitoid/gneissic, low-grade metamorphic, and extrabasinal carbonate rock fragments, as well as by picotite and glaucophane.

The application of detailed petrographic observations for discriminating paleo- vs. neovolcanic and penecontemporaneous vs. noncoeval terrigenous sands lead to a substantial revision of the geodynamic interpretation of the Thrace Basin, formerly considered a forearc basin. A significant penecontemporaneous volcanic component is common in the Upper Eocene–Lower Oligocene section and can be related to extensive post-collisional volcanism following the closure of the Vardar–İzmir–Ankara ocean. The coexistence of pure neovolcanic layers (crystal tuffs and cinerites) and hybrid arenites rich in penecontemporaneous carbonate grains with sands derived from a continental basement and ophiolitic suites indicates the presence of episutural basins where shallow-water carbonates were deposited on top of the exhuming subduction–accretion prism. These carbonates were mixed with penecontemporaneous neovolcanic and terrigenous components and redeposited in deeper marine environments.

© 2011 Elsevier B.V. All rights reserved.

### 1. Introduction

Several authors have linked specific plate-tectonic settings to the mineralogical composition of sands and sandstones (e.g., Dickinson, 1970, 1985; Crook, 1974; Dickinson and Suczek, 1979; Ingersoll and Suczek, 1979; Valloni and Maynard, 1981; Dickinson et al., 1983; Mack, 1984; Valloni and Zuffa, 1984; Valloni, 1985; Garzanti et al., 2007). In spite of (i) some limiting factors, like modifications occurring during weathering, sediment transport, deposition, and

diagenesis (see, for example, the papers in Basu, 1993 and Zuffa, 1985 and Johnsson), and (ii) other important critical remarks to be taken into consideration (e.g. Zuffa, 1991; Weltje, 2006), these broad correlation schemes have been evaluated extensively, and sandstone detrital modes are now commonly employed to determine, in conjunction with other basin-analysis techniques, the plate-tectonic setting of ancient terrigenous successions (for a review, see Garzanti et al., 2007).

Calibrated procedures for recognizing and classifying sand/sandstone grain types (particularly carbonate and volcanic grains) are critical in reconstructing source/basin paleogeography and assessing evolutionary trends through time. In particular, the analytical procedure for point counting of arenite framework requires fundamental attributes of grains to be taken into account, like composition (carbonate

\* Corresponding author.

E-mail addresses: [azzurra.datri@unibo.it](mailto:azzurra.datri@unibo.it) (A. d'Atri), [giangaspazuffa@unibo.it](mailto:giangaspazuffa@unibo.it) (G.G. Zuffa), [william.cavazza@unibo.it](mailto:william.cavazza@unibo.it) (W. Cavazza), [okay@itu.edu.tr](mailto:okay@itu.edu.tr) (A.I. Okay), [g.divincenzo@igg.cnr.it](mailto:g.divincenzo@igg.cnr.it) (G. Di Vincenzo).

versus non-carbonate grains), spatial relationships (intra-basinal versus extrabasinal grains), and time relationships (grains coeval or non-coeval with respect to the basin fill) (e.g. Zuffa, 1980, 1987; Ingersoll et al., 1987; Critelli and Ingersoll, 1995).

Clastic successions characterized by either (i) compositionally hybrid beds or (ii) alternating strata of siliciclastic and penecontemporaneous carbonate-clastic composition may indicate, respectively, (i) the presence of marine shallow-water 'sediment parking areas' where extrabasinal and intra-basinal grains can mix before being resedimented (e.g. Fontana et al., 1989), and (ii) distinct terrigenous and intra-basinal sources playing an independent role in supplying the depocenter (e.g. Gandolfi et al., 1983, 2007). Moreover, the detection of neovolcanic and paleovolcanic grains within the same arenite succession is crucial for a correct interpretation of the geotectonic setting in which sediments were deposited (e.g. De Rosa et al., 1986; Critelli and Ingersoll, 1995; Hathway and Kelley, 2000; Pal et al., 2005). Thus, a thorough knowledge of the composition, origin, and age of arenite grains is critical in unraveling source/basin paleogeography and tracing its evolution through time. As a final point, we must bear in mind that source area reconstructions should not be conducted with gross compositional data alone, but need to be supported by other lines of evidence (heavy minerals, paleocurrents, facies relations, etc.).

This paper illustrates how detailed definition of sandstone detrital modes (including heavy-mineral analysis, paleocurrent analysis, and the study of sedimentological facies relationships) can discriminate not only the overall plate-tectonic setting of terrigenous successions, but also pinpoint significant within-basin provenance variations, thus providing important elements to constrain (i) the sediment dispersal pattern, (ii) the three-dimensional geometry of petrographic lithosomes, and (iii) the overall basin evolution. To this end, we studied the sandstone petrography of the Eocene–Oligocene sedimentary succession of the southern Thrace Basin (northwestern Turkey and northeastern Greece). This portion of the basin was chosen as the study area because recent studies have constrained the paleoenvironmental/paleostructural setting and the chronostratigraphy of the basin fill (Okay et al., 2010; Özcan et al., 2010), thus integrating a large wealth of preexisting data, both from surface and subsurface studies (e.g. Doust and Arıkan, 1974; Şengör, 1979; Önal, 1986; Sümengen and Terlemez, 1991; Görür and Okay, 1996; Turgut and Eseller, 2000; Yaltırak and Alpar, 2002; Okay et al., 2004).

## 2. Geological setting

The Thrace Basin is a complex system of depocenters located between the Rhodope–Strandja Massif to the north and west and the Biga Peninsula to the south (Fig. 1). The southern margin of the basin is now covered by the Marmara Sea and deformed by the North Anatolian Fault. The Thrace Basin is the largest and thickest Tertiary sedimentary basin of the eastern Balkan region and constitutes an important hydrocarbon province (Turgut et al., 1991; Turgut and Eseller, 2000; Siyako and Huvaz, 2007). The older part of the basin fill crops out along the basin margins but it is covered by Plio-Quaternary deposits in the basin center (Siyako, 2006). In this area, subsurface data is abundant as Türkiye Petrolleri Anonim Ortaklığı (TPAO) has drilled more than 350 wells and acquired in the 80s and 90s a fairly dense network of seismic lines.

Most Thrace Basin strata range from the Lower Eocene (Ypresian) to the Upper Oligocene. Maximum total thickness, including the Neogene–Quaternary succession, commonly reach 5000 m and goes up to 9000 m in a narrow depocenter bounded by strike-slip faults (Yıldız et al., 1997; Turgut and Eseller, 2000; Siyako and Huvaz, 2007). In terms of volume, most of the Eocene–Oligocene sedimentary succession is made of basin–plain turbidites (Aksoy, 1987; Turgut et al., 1991). Sedimentation along the basin margins was characterized by carbonate deposits during the Eocene and by deltaic bodies prograding towards the basin center in the Oligocene (Sümengen et al., 1987;

Sümengen and Terlemez, 1991). The western margin of the basin, in Greek and Bulgarian territory, was characterized already in the Eocene by a series of coarse-grained fan-deltas prograding eastward and feeding the depocentral basin–plain turbidites (Caracciolo et al., 2007a, b).

The Thrace Basin lies across a geodynamically complex area characterized by three juxtaposed lithospheric blocks (terrane) distinguishable as to lithology, structural configuration, and geological evolution: the Rhodope–Strandja crystalline massif, the İstanbul Zone, and the Sakarya Zone (Fig. 1). (1) The Rhodope–Strandja massif has Laurasian affinity and it is composed of Variscan continental crust, Mesozoic metasedimentary rocks, and fragments of oceanic crust (Burg et al., 1996). This assemblage suffered repeated phases of crustal thickening and exhumation during the Cretaceous and early Tertiary (e.g. Krohe and Mposkos, 2002). The main phase of deformation occurred in the Maastrichtian–early Paleogene following the closure of the Vardar Ocean (Stampfli and Borel, 2004). A widespread extensional regime active from mid-Eocene time induced the exhumation of the Rhodopian core complexes (e.g. Bonev and Beccaletto, 2007). (2) Located at the southwestern margin of the Black Sea, the İstanbul Zone is a continental fragment about 400 km long and 70 km wide. It comprises a Precambrian crystalline basement and a fairly complete Ordovician–Carboniferous sedimentary cover which was deformed during the Variscan orogeny (Görür et al., 1997; Okay et al., 2011). Its stratigraphic, paleobiogeographic, and paleomagnetic characters show a marked Laurasian affinity. It was proposed that this continental fragment rifted off the Odessa shelf and drifted southward during the opening of the western Black Sea backarc basin in the Cretaceous (Görür and Okay, 1996). (3) The Sakarya Zone, approximately 1500 km long and 120 km wide, is a continental block separated from the Rhodope–Strandja crystalline massif and the İstanbul Zone by the so-called Intra-Pontide suture (Şengör and Yılmaz, 1981). The basement of this terrane is made of amphibolite-facies metamorphic rocks visible in a few tectonic windows of limited areal extent (e.g. Okay et al., 2008; Cavazza et al., 2009). In the Paleogene, the Sakarya Zone collided with the Anatolide–Tauride terrane of African affinity to the south following the closure of the İzmir–Ankara ocean (Okay and Tüysüz, 1999; Stampfli and Borel, 2004).

Juxtaposition of the İstanbul and Sakarya Zones along the Intra-Pontide suture occurred in pre-Cenozoic time, although the exact timing has not been yet clearly defined. The westward continuation of the Intra-Pontide suture into the Marmara Sea is controversial. Scattered outcrops of the ophiolitic Çetmi mélangé in the Biga peninsula have been interpreted as marking the Intra-Pontide suture between the Sakarya Zone to the southeast and terrains of Rhodopian affinity to the northwest (Siyako et al., 1989; Okay and Tüysüz, 1999; Beccaletto et al., 2005). Stampfli and Hochard (2009) date the formation of the suture in the Biga peninsula at 200–180 Ma (Late Triassic–Early Jurassic) despite the fact that the blocks and the matrix composing the mélangé reach up to the Early Cretaceous (Beccaletto, 2004).

Juxtaposition of the Sakarya and Anatolide–Tauride terranes occurred between the Late Cretaceous and the Paleogene following northward subduction and closure of the Vardar Ocean and its continuation to the east, the İzmir–Ankara ocean (Okay and Tüysüz, 1999; Stampfli and Hochard, 2009). The transition between the collisional tectonic regime following the closure of these oceanic realms and the extensional regime characterizing the Neogene evolution of the Aegean and peri-Aegean regions is complex and relatively poorly known (e.g. Burchfiel et al., 2000; Bonev, 2006; Bonev and Beccaletto, 2007;). The Thrace Basin developed during this transitional tectonic regime.

Contrasting hypotheses have been put forward to explain the origin and the evolution of the Thrace Basin. (1) Keskin (1984) and Perinçek (1991) considered this basin as intramontane in nature. (2) Turgut et al. (1991) and Tüysüz et al. (1998) proposed a transtensional post-collisional origin following the closure of the Intra-Pontide Ocean. (3)

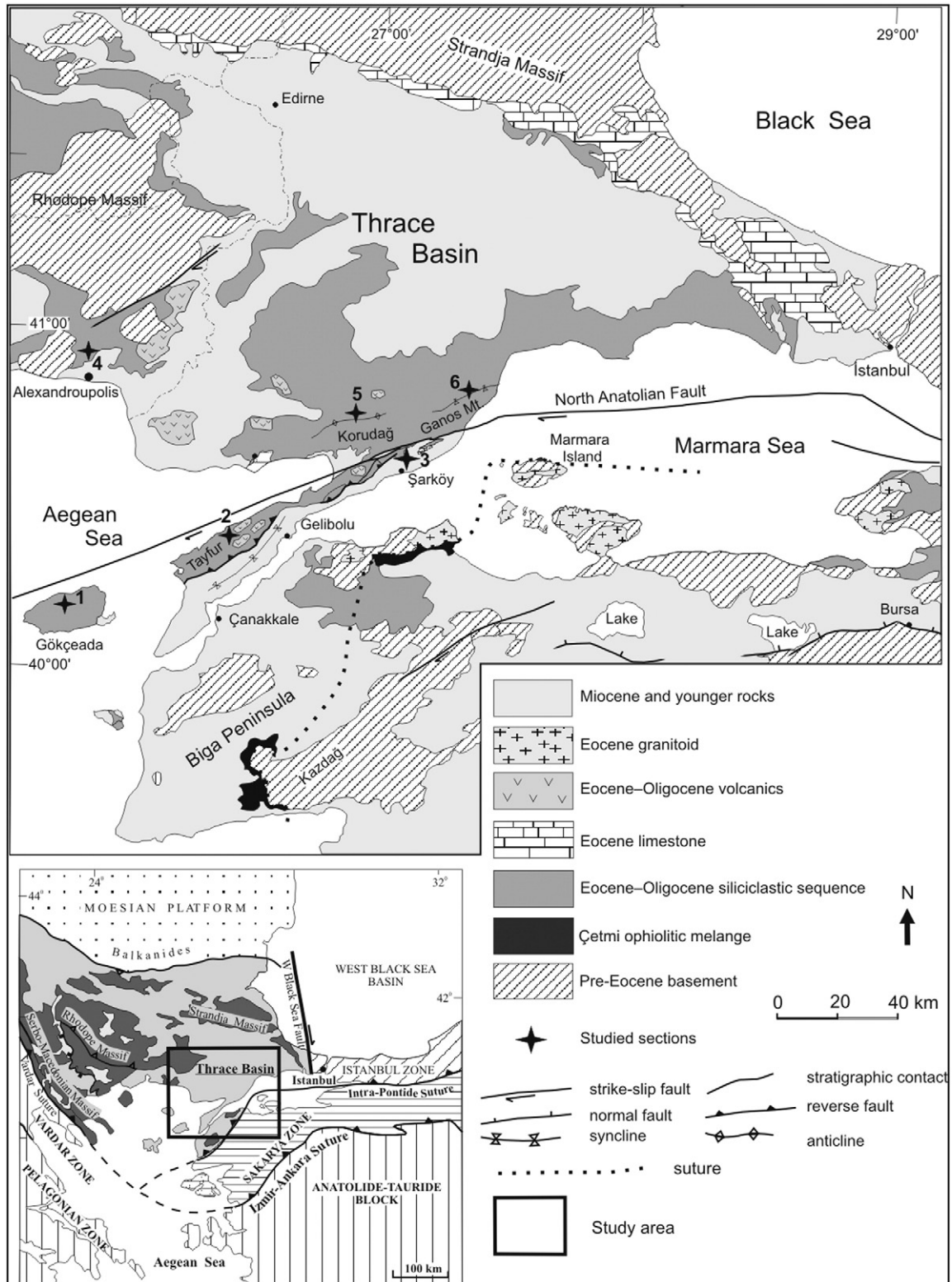


**Fig. 1.** Tectonic map of the Thrace region (modified from Okay et al., 2010) showing the Eocene–Oligocene sedimentary outcrops, the Upper Cretaceous ophiolitic mélange and the pre-Eocene basement. Numbers indicate the studied stratigraphic sections. The smaller box (left) show position of Thrace basin respect to main tectonic domains.

Görür and Okay (1996) suggested a forearc location between a subduction–accretion complex to the south and a volcanic arc to the north. (4) Şen (2002) championed a flexural origin due to the loading induced by backthrusts related to the İzmir–Ankara suture.

### 3. Stratigraphy of the southern Thrace Basin

The stratigraphy of the southern Thrace Basin is somewhat different north and south of the Ganos segment of the North Anatolian

Fault, which also separates two different basement types (e.g., [Doust and Arikan, 1974](#); [Sümengen and Terlemez, 1991](#); [Turgut et al., 1991](#); [Siyako and Huvaz, 2007](#); [Okay et al., 2010](#)). The basement north of the Ganos Fault is composed of low-grade metamorphic rocks belonging to the circum-Rhodope belt and it is covered by a shallowing upward succession of Middle–Upper Eocene distal to proximal turbidites, overlain by shelfal, deltaic, and continental facies of Oligocene age ([Okay et al., 2010](#)). Conversely, the basement south of the Ganos Fault consists of an ophiolitic mélangé (Çetmi mélangé, [Okay et al., 1991](#); [Beccaletto et al., 2005](#); [Okay et al., 2010](#)) with serpentinite, metadiabase and blueschists. The Eocene succession overlying the Çetmi mélangé contains thick olistostromes and large olistoliths derived from the mélangé ([Okay et al., 2010](#)). Six stratigraphic sections were studied and sampled ([Fig. 2](#)): three to the south and three to the north of the Ganos Fault. They represent the better exposed and most continuous sections available in the southern part of the Thrace Basin. Their main characteristics are described below.

### 3.1. Gökçeada

The composite section shown in [Fig. 2](#) is about 1500 m thick and does not include the topmost, thick Oligocene pyroclastics and lava

flows. From base to top, the section comprises [see [Temel and Çiftçi, \(2002\)](#), for a detailed description]:

- a succession of continental-to-deltaic shale and sandstone with subordinate conglomerate beds; this succession correlates with the Karaağac and Fıçitepe formations cropping out extensively nearby in the Gelibolu Peninsula ([Siyako and Huvaz, 2007](#)), is about 500 m thick, and is of ?Early–Middle Eocene age;
- shallow-marine carbonate and fine-grained sandstone (total thickness: ca. 150 m) with nummulitids, alveolinids, corals, and algae (Middle Eocene, Soğucak Formation, [Özcan et al., 2010](#); [Siyako and Huvaz, 2007](#));
- complex alternation of shale and coarse-grained sandstone beds with erosive basal contacts, clay chips, and bed amalgamation; this unit becomes progressively sandier upsection and was deposited in a slope-to-delta front environment, as shown by abundant slump structures (ca. 700 m; Upper Eocene–Lower Oligocene);
- medium to coarse grained sandstone of deltaic environment (> 100 m; Osmancik Formation; Lower–Middle Oligocene; [Atalik, 1992](#));
- fluvial sandstone, shale, and conglomerate (<100 m; Armutburnu Formation; Upper Oligocene; [Siyako et al., 1989](#)) (not shown in [Fig. 2](#)).

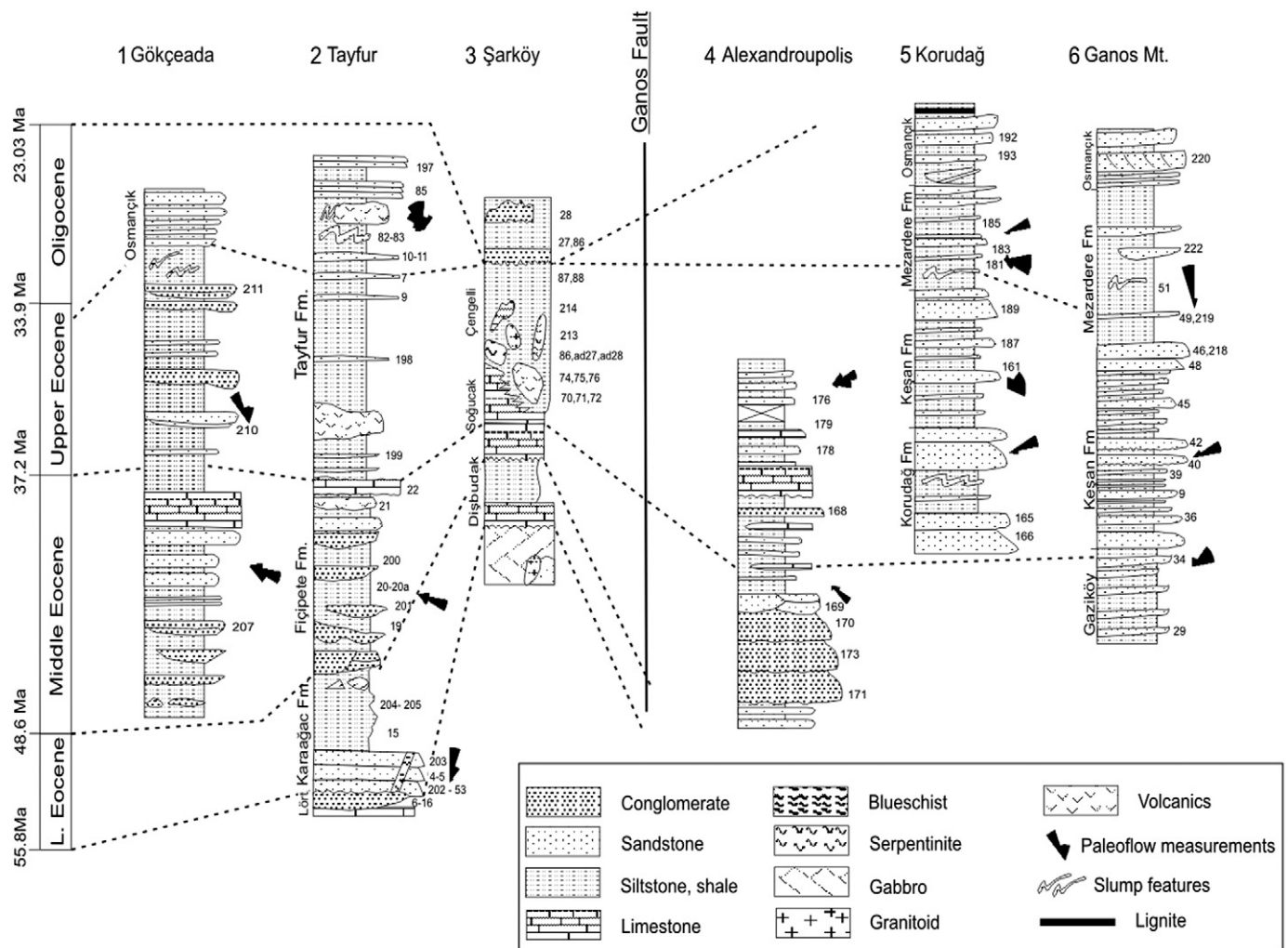


**Fig. 2.** Stratigraphic sections and correlations in the studied areas, from west to east, north and south of Ganos Fault respectively. For section location see numbers in [Fig. 1](#). Sample position and paleoflow measurements are shown in each section. Geological time scale from [Gradstein et al. \(2004\)](#).

### 3.2. Tayfur

This section is >3000 m thick (Fig. 2) and crops out extensively between Karaağac Bay (Saros Gulf) and Tayfur dam. The stratigraphic units comprising this section are:

- a relatively small outcrop of Cretaceous–Paleocene pelagic limestone (Lört Formation; Önal, 1986), traditionally considered as the base of the section and recently reinterpreted by Okay et al. (2010) as a large olistolith within the turbidites of the Karaağac Formation;
- a ca. 800 m thick section of deep-marine turbiditic sandstone and shale grading upward into hemipelagics, prodelta shale, and delta-front sandstone (Karaağac Formation) (Lower Eocene; Sümengen and Terlemeç, 1991; Temel and Çiftçi, 2002; Siyako and Huvaz, 2007);
- alternating fluviatile mudrock, sandstone, and conglomerate (red beds) (ca. 800 m; Fiçtepe Formation; Middle Eocene; Kellog, 1973);
- nummulitic limestone overlying unconformably the red bed succession (20–30 m; Soğucak Formation; Bartonian, Özcan et al., 2010);
- fine-grained and thin bedded slope turbidites (Tayfur Formation; Önal, 1986) with abundant slump features cropping out extensively south of Tayfur village. A significant penecontemporaneous volcanoclastic component is present. A large vitric tuff olistolith occurs in the upper part of this unit. This formation is here interpreted as having been deposited in a slope environment. Two samples from the tuff (TU-52 and TU-84) were analyzed by the  $^{40}\text{Ar}$ – $^{39}\text{Ar}$  method in order to constrain the time of deposition. Age data are summarized in Table 1. Analytical techniques were those described in detail in Di Vincenzo et al. (2003, 2010). Biotite separates from both samples were first analyzed by the laser step-heating technique on milligram-sized sample, and yielded total gas ages of ~32.5 and ~30.9 Ma for TU-52 and TU-84, respectively (Table 1), and discordant age spectra with an overall asymmetric hump shape. These shapes may arise from either contamination by extraneous Ar (excess or inherited Ar) or from analytical artifact, namely redistribution of Ar isotopes during sample irradiation between biotite and interlayered chlorite (e.g., Di Vincenzo et al., 2003). In order to ascertain intergrain Ar isotope variability and to verify the presence of a correlation between age and atmospheric Ar content and – in turn – with potential alteration, biotite concentrates were also analyzed through the laser total fusion technique on single grains. Ages of biotite TU-52 span a large interval of ~30.4 to ~39 Ma and lack a clear correlation with the atmospheric Ar content, thus making the analytical artifact as a cause for hump-shaped profiles a less likely possibility. The six youngest ages overlap within analytical errors and yield an error-weighted mean of  $30.64 \pm 0.24$  Ma (Table 1). Total fusion ages of biotite TU-84 define a narrower time interval, ~30.1 to

31.2 Ma. Nine out of fourteen analyses yield ages overlapping within errors and a mean of  $30.42 \pm 0.21$  Ma, indistinguishable at the  $2\sigma$  confidence level from that of biotite TU-52. A comparable age was also obtained from a step-heating experiment on a feldspar concentrate of sample TU-84, which gave a concordant segment representing 68% of the  $^{39}\text{Ar}_K$  released with an error-weighted mean of  $30.22 \pm 0.20$  Ma (Table 1). We therefore assign intergrain age variability of biotite to heterogeneously distributed extraneous Ar and interpret the age from the concordant segment of feldspar TU-84 as a reliable eruption age of the tuff. The abundance of penecontemporaneous volcanoclastic detritus throughout the upper Tayfur Fm. (see Section 6) points to a virtual coincidence between tuff age and depositional age of the upper Tayfur Fm. This new radio isotopic dating indicates that the Tayfur Fm. spans a longer time interval than previously thought (Önal, 1986; Temel and Çiftçi, 2002).

### 3.3. Şarköy

The Şarköy section is the result of recent mapping (Okay et al., 2010) and micropaleontological dating (Özcan et al., 2010) that resulted in a substantial revision of the stratigraphy of the area. Three stratigraphic units comprise this section:

- a thin and local Lower Eocene carbonate–siliciclastic sequence, called the Dişbudak series (Ypresian), consisting of a transgressive succession of pebbly sandstone grading upward into sandy and then nodular limestone, in turn overlain by marl and shale (Okay et al., 2010). The Dişbudak series is an upward deepening and upward fining transgressive succession (Okay et al., 2010), which is unconformably overlain by the Upper Bartonian Soğucak Formation (see below). Similar Lower Eocene sequences are described from Bozcaada (Varol et al., 2007) and northwest Turkey (Özgörüç et al., 2009). The entire Lutetian and most of the Bartonian section are missing, indicating deep erosion before the Late Bartonian marine transgression marked by deposition of the Soğucak Formation. The Dişbudak series represents a marine transgression before the initiation of major subsidence in the Thrace Basin. Its deposition was followed by a major phase of uplift and erosion.
- Upper Bartonian to Lower Priabonian (SBZ 19) (Özcan et al., 2010) Soğucak Formation unconformably overlying the Dişbudak series. It consists of a 200 m thick succession of thickly bedded to massive, white, shallow-marine limestone with algae, corals, bryozoa, and foraminifera. The top of the Soğucak Formation has an Early Priabonian age (SBZ 19) (Özcan et al., 2010).
- a turbidite succession with large olistoliths and thick olistostromes (ca. 1000 m; Çengelli Formation; Upper Eocene–Lower Oligocene,

**Table 1**  
Summary of  $^{40}\text{Ar}$ – $^{39}\text{Ar}$  results.

Sample	Extraction technique	Phase analyzed	Fraction (mm)	sample	Total number of analyses	Total gas age (Ma)	$\pm 2\sigma$	Remarks	Age (Ma)	$\pm 2\sigma$	MSWD	# of analyses
TU-52	Step-heating	Biotite	0.25–0.50	~2 mg	12	32.47	0.20	Concordant segment representing 41.7% of $^{39}\text{Ar}$ released (steps 8 to 13), considered unreliable Range: $30.39 \pm 0.36$ to $38.7 \pm 1.1$ Ma	33.59	0.22	1.12	4
TU-52	Total fusion	Biotite	0.25–0.50	Single grain	11	32.43	0.25		30.64	0.24	0.86	6
TU-84	Step-heating	Biotite	0.18–0.30	~2 mg	13	30.94	0.23	Concordant segment representing 46.5% of $^{39}\text{Ar}$ released (steps 8 to 13), considered unreliable Range: $30.11 \pm 0.44$ to $31.23 \pm 0.41$ Ma	30.88	0.19	0.92	6
TU-84	Total fusion	Biotite	0.18–0.30	Single grain	14	30.69	0.20		30.42	0.21	0.84	9
TU-84	Step-heating	Feldspar	0.30–0.50	50 grains	7	29.83	0.19	Concordant segment representing 67.9% of $^{39}\text{Ar}$ released	30.22	0.20	0.56	6

#: error-weighted means. MSWD: mean square of weighted deviates. Uncertainties are  $2\sigma$  internal errors, including in-run statistics, uncertainties in the discrimination factor, interference corrections, procedural blanks and flux monitor. Lat/long for both samples: N40°23'11.9" E26°29'20.4".

Okay et al., 2010). Most of this unit is made of thin-bedded turbidites (TBT) with abundant slump features indicative of a slope environment. Two types of blocks occur in the Upper Eocene mass flows: (a) ophiolitic mélange, (b) Eocene shallow-marine limestone. The occurrence of composite blocks indicates that the subduction/accretion complex from which the ophiolitic detritus was derived was locally overlain by Upper Eocene neritic limestone. Paleontological data from the Çengelli Formation (Özcan et al., 2010) show no measurable difference between the age of the siliciclastic turbidites and the Eocene limestone blocks (Priabonian; 37–34 Ma), thus indicating that the limestone was intrabasinal and penecontemporaneous to turbidite deposition. The source was quite close as blocks are up to 1 km across and include fragile rock types such as serpentinite or greywacke-shale, which cannot be transported unbroken over great distances. As there are no olistostromal Eocene facies north of the Ganos Fault the source area must have been located to the south. Şengör and Yılmaz (1981) regarded the ophiolitic mélange outcrops north of Şarköy as marking the location of the Intra-Pontide suture. This interpretation is challenged by Okay et al. (2010) who mapped the ophiolitic olistoliths and olistostromes as sedimentary units within the Çengelli Formation.

### 3.4. Alexandroupolis

The geology of the region north of Alexandroupolis in NE Greece is characterized by a thick Tertiary sedimentary succession nonconformably overlying the metasedimentary rocks (mostly phyllite, but including also metaconglomerate, metasandstone, and marble) of the circum-Rhodopian belt. Chronostratigraphic control on this thick succession is still relatively poor. The following description is from Caracciolo (2009) and Maratos et al. (1977), integrated by our own field observations. Four stratigraphic units comprise the Tertiary succession:

- the base of this section is characterized by coarse grained, poorly organized conglomerate and by subordinate very coarse grained sandstone of Lutetian age. Conglomerate clasts are granite, gneiss, amphibolite, and marble. These basal deposits are capped by coarse grained sandstone with large-scale trough and epsilon crossbeds. This portion of the section is interpreted as an alluvial fan/fan-delta succession evolving upward into braided river and deltaic deposits.
- a mostly pelitic succession, about 500 m thick, with thin sandstone and carbonate beds. This unit is interpreted as shelf mudrock interbedded with siliciclastic and carbonate shelf turbidites. Local, lenticular coal seams are found in the top portion of this stratigraphic unit and are similarly interpreted as the result of redeposition of continental/coastal carbonaceous matter on the continental shelf.
- an 80–100 m thick tabular body of marly limestone (*Em.mk* of Maratos et al., 1977) with nummulitids, calcareous algae, foraminifera, corals, echinoids, and bivalves (Upper Lutetian–?Priabonian, Maratos et al., 1977). This unit covers with a slight angular unconformity all of the underlying units including the basement and crops out to the east over a distance in excess of 30 km (Papadopoulos, 1980).
- a 500 m thick succession of deep-marine thin bedded siliciclastic turbidites of Late Eocene age with rare carbonate allodapic beds. Volcaniclastic layers and lava flows were not measured in this section but are common in age-equivalent deposits nearby (e.g. Papadopoulos, 1980).

### 3.5. Korudağ

This is a composite section as the lower portion was measured south of Keşan along the road to Saros Bay whereas the upper portion was measured in the northeastern outskirts of Keşan and along the Malkara-İpsala freeway immediately to the north. Its composite

nature and scattered outcrops make a coherent paleoenvironmental interpretation of this stratigraphic section difficult. Four stratigraphic units comprise this section:

- a thick succession of thick-bedded siliciclastic turbidites (>1000 m; Korudağ Formation; Upper Eocene) alternating with horizons of thin-bedded turbidites with abundant slump features. Paleocurrent directions and slump features all point to easterly paleocurrents and paleoslope. This formation is interpreted as the result of deposition along a continental slope. The thick sandstone horizons represent the fills of broad channels cut into slope deposits (thin-bedded turbidites with slumps).
- another thick succession of siliciclastic turbidites (>1000 m; Keşan Formation; Upper Eocene, Siyako and Huvaz, 2007; Sümengen and Terlemez, 1991) overlies conformably the Korudağ Formation. Sandstone/shale ratio is lower than that of the Korudağ Formation. A few layers rich in volcaniclastic detritus are present. Paleoflow directions are generally from west to east, parallel to the Ganos Fault. The Keşan Formation is interpreted as the result of deposition from gravity flows in a proximal basin plain and base-of-slope environment. Characteristic depositional-lobe and lobe-fringe sequences are common.
- the Korudağ and Keşan formations are followed by Upper Eocene–Lower Oligocene shale of Mezardere Formation, made up of ca. 750 m of mudrock with intercalations of fine grained, rippled sandstone interbeds. Mudrocks contain remnants of diatoms and shallow-marine gastropods, ostracods, and bivalves (Doust and Arikan, 1974). This formation was most likely deposited in a shelf environment, with a vertical trend from outer shelf to prodelta deposits.
- thickly bedded, coarse grained sandstone, locally with large-scale cross beds (>500 m; Osmançık Formation; Oligocene). The top of this unit shows intercalation of conglomerate beds and coal seams with plant fragments. This formation represents deposition in a sand-rich deltaic environment (Atalik, 1992; Doust and Arikan, 1974).

### 3.6. Ganos Mountain

This stratigraphic section can be studied along the northern shores of the Marmara Sea from the eastern end of the Ganos Fault just north of Gaziköy to the town of Barbaros. Overall, the stratigraphy is very similar to that of the Korudağ section (Fig. 2), with a general middle Eocene-to-Oligocene regressive trend from deep-marine turbidites to continental deposits. Individual stratigraphic units of the Ganos Mt. section, as well as their thicknesses and sedimentological features, can be correlated with those of the Korudağ section, with two exceptions:

- an 850 m thick succession of thin-bedded basin-plain turbidites (Gaziköy Formation; middle Eocene, Siyako and Huvaz, 2007) with a few volcanic tuff layers of andesitic composition (Yılmaz and Polat, 1998) and submarine lava flows. This is the oldest formation cropping out north of the Ganos Fault.
- a Korudağ Formation is not recognized as an independent unit and the time-equivalent section is included in a much thicker Keşan Formation.

## 4. Sampling and methods

A total of 132 medium- to coarse-grained arenite samples were collected from the study area along the described stratigraphic sections (for exact sample locations, see d'Atri, 2010). Thin sections were made and stained with sodium cobaltinitrite and alizarine red S, to facilitate identification of potassium feldspar and carbonate grains (Chayes, 1952; Lindholm and Finkelmann, 1972). Quantitative petrographic analyses were performed on 77 thin sections for gross composition by using an integrated Gazzi–Dickinson–Zuffa point

counting method (Gazzi, 1966; Dickinson, 1970; Gazzi et al., 1973; Zuffa, 1980, 1985, 1987; Ingersoll et al., 1984, 1987; Critelli and Ingersoll, 1995). This procedure allows: (i) to minimize errors due to dependence of rock composition on grain size, (ii) to record both which mineral is underneath the cross hair and the type of rock fragment in which the mineral is located, (iii) to obtain the best possible separation between extrabasinal and intrabasinal carbonate grains, and (iv) to distinguish between paleovolcanic (derived by erosion of old volcanic rock suites) and neovolcanic grains (derived from active volcanism located either inside or outside of the basin). A minimum of 300 grains were counted and divided into four main groups: NCE (non-carbonate extrabasinal), CE (carbonate extrabasinal), NCI (non-carbonate intrabasinal), CI (carbonate intrabasinal). The compositional classes adopted are those proposed by Cibin and Di Giulio (1996).

Considering the scarcity of intrabasinal detrital components, point-counting results were plotted on a QF(L+CE) ternary diagram (Fig. 4). Such diagram takes into consideration the entire spectrum of terrigenous framework grains, including carbonate lithoclasts that are ignored in the standard QFL diagram of Dickinson and Suczek (1979).

Quantitative petrographic study also included the analyses of the heavy-mineral concentrates obtained from 40 samples. Sandstone samples were disaggregated using standard laboratory techniques; heavy minerals were then separated with tetrabromoethane (density 2.967 g/cm<sup>3</sup>). Following separation, non-permanent grain mounts (Gazzi et al., 1973) were made by sprinkling the grains onto a glue-covered microscope slide. 1-iodonaphthalene (refraction index 1.701) was then dropped onto the sample and the slide was topped with a cover glass. Optical counting of heavy minerals was performed by the ribbon method. 200 to 300 transparent grains were counted for each sample, not including anhydrite, barite, and Mg/Fe-carbonate.

The integrated results of the analyses of sandstone gross composition, rocks fragments, and heavy minerals – together with the analysis of paleocurrent indicators – allowed the discrimination of two compositional petrofacies (see Section 6).

## 5. Description of framework and interstitial components

### 5.1. NCE (non-carbonate extrabasinal grains)

This group comprises quartz, feldspars, coarse- and fine-grained rock fragments, micas, and heavy minerals. Quartz occurs as monocrystalline and polycrystalline grains, and as a constituent of plutonic–gneissic, low-grade metamorphic, and volcanic rock fragments. Feldspars are present either as plagioclase or K-feldspars. Plagioclases occur as single crystals, both as neovolcanic grains (pristine euhedral crystals) with albite-type twinning and/or zoning (Fig. 3B, C, E), and as paleovolcanic grains generally sericitized or replaced by calcite. Plagioclase grains are also found in plutonic–gneissic, phyllitic, and volcanic rock fragments. K-feldspars, with the exception of the Alexandroupolis stratigraphic section, are less abundant than plagioclase and mostly occur as single crystals or within plutonic–gneissic rock fragments. They are often altered into kaolinite and illite or replaced by calcite. Biotite, muscovite, and chlorite are mostly found in metamorphic rock fragments (gneiss, phyllite, and chlorite schists) and as single crystals. Aphanitic rock fragments comprise metamorphic, volcanic, and sedimentary types. The dominant metamorphic lithic grains are phyllites and slates. Serpentinite, chlorite-schist, and serpentine-schists, related to ophiolitic suites, can be present in considerable amounts. Volcanic rock fragments span the whole compositional spectrum, including acidic, intermediate, and basic types. Acidic lithics display phenocrysts of quartz and plagioclase in a microgranular felsitic groundmass. Intermediate and basic lithics have microlithic and lathwork, commonly chloritized, texture. Distinctive diabase rock fragments are present (Fig. 3D). Sedimentary rocks fragments are represented by siltstone and chert.

### 5.2. CE (carbonate extrabasinal grains)

Carbonate terrigenous grains encompass micritic and microsparitic limestone and minor dolostone, from fine to coarse-grained. They are relatively abundant (ca. 5%) in the Karaağac Formation at the base of the Tayfur section, whereas they are virtually absent higher up in the same section and in the Alexandroupolis section. In all other sections they average 2% of the framework grains. In a few cases, carbonate extrabasinal grains could be tied to specific rock units in the sediment source area as, for example, in the Tayfur section where carbonate lithoclasts contain tintinnids tests (Fig. 3A).

### 5.3. CI (carbonate intrabasinal grains)

This group is chiefly represented by bioclasts and biosomes of nummulitids, algae, bryozoans, and foraminifers. Peloids, ooids (e.g. Fig. 3B) and minor intraclasts are also present. Carbonate intrabasinal grains are abundant in the Gelibolu stratigraphic section where they make up to 8% of the total framework grains.

### 5.4. NCI (non-carbonate intrabasinal grains)

The components of this group occur only in traces and are represented by grains of iron oxides, glaucony, and by rip-up clasts.

### 5.5. Interstitial components

The matrix consists mostly of silt-size grains of quartz, feldspars, and mica/chlorite. The cement is mostly microsparitic to sparitic low-Mg calcite with a few samples exhibiting a patchy calcite texture. Early mechanical compaction produced intense deformation of more ductile grains and reduced significantly primary porosity. As a result, modal percentage of calcite cement ranges only between 5 and 8%. Minor quantities of kaolinite, illite, and chlorite occur locally as pore-filling or pore-lining cement. Quartz and feldspars overgrowths are a subordinate component of cement. Calcite replacement of dissolution-prone framework grains (mostly feldspars) is locally common, but never strong enough to hamper the identification of grains during point counting.

## 6. Results of sandstone petrographic analyses

The results of sandstone modal analyses indicate that sandstones of the southern Thrace Basin range compositionally between lithic arkoses and arkosic litharenites of medium to low compositional maturity. (For the original analytical data, see d'Atri, 2010.) All samples are prevalently made up of siliciclastic terrigenous grains. Other characteristic features include a high plagioclase/K-spar ratio and a predominance of low-grade metamorphic (phyllite and slate) and volcanic lithic fragments within the rock fragments population. Some samples have carbonate intrabasinal and extrabasinal components represented by bioclasts and fine-grained carbonate rock fragments, respectively.

Zircon, tourmaline, rutile, and garnet constitute >50% of the heavy-mineral fraction and are present in all samples. Picotite is present in all samples (20% on average) except those from the Alexandroupolis section, and clearly indicates a provenance from ophiolitic rocks. Numerous other heavy minerals such as clinopyroxene, clinopyroxenes, monazite, epidotes, chloritoid, kyanite, staurolite, and glaucophane are present in very low quantities or in traces. In particular, augite characterizes the upper part of the Tayfur stratigraphic section and epidotes and glaucophane characterize the Şarköy section (see d'Atri, 2010, for further details). Garnets from some samples of the Korudağ and Ganos Mt. sections show well developed “faceting” indicating diagenetic overgrowth (Morton and Hallsworth, 1999). Pristine euhedral anatase is present in several samples as an authigenic mineral phase.

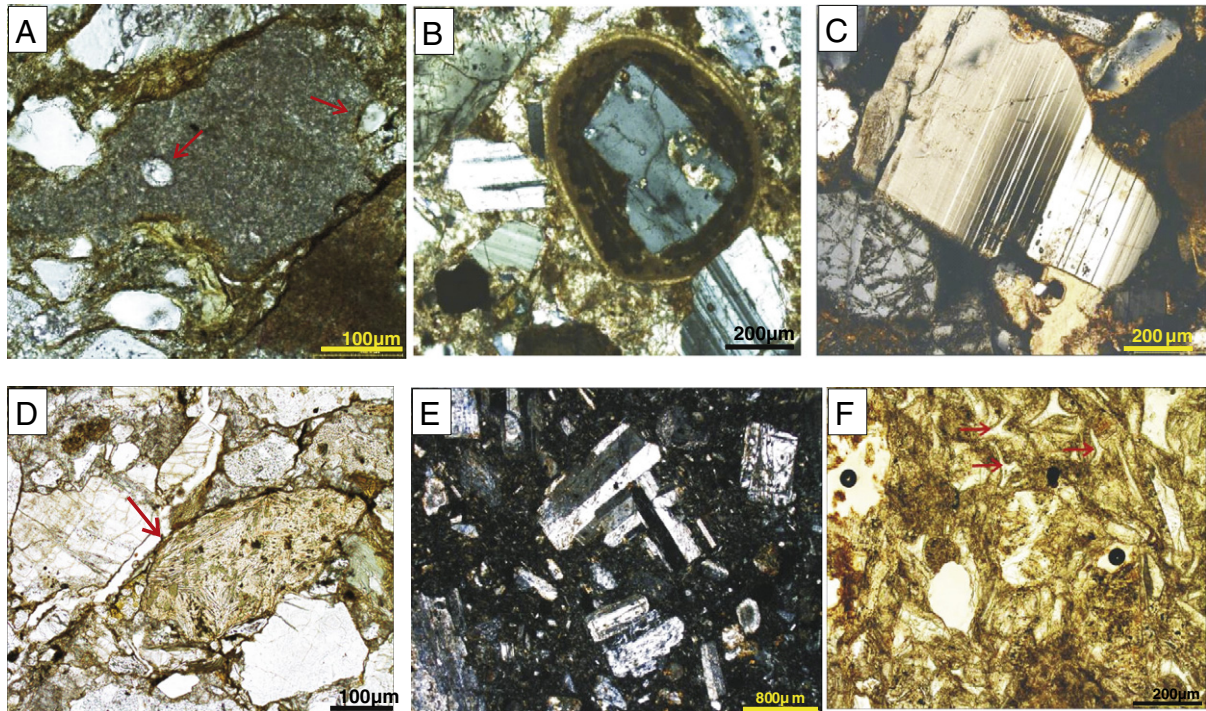


**Fig. 3.** Thin section photomicrographs showing different grain types and petrofacies of Thrace Basin arenites. (A) Extrabasinal carbonate grain: micritic limestone with Tintinnid tests (red arrows); southern petrofacies, crossed nicols. (B) Oolitized feldspar grain; southern petrofacies, crossed nicols. (C) Neovolcanic plagioclase; southern petrofacies, crossed nicols. (D) Diabase lithic grain (red arrow), northern petrofacies, polarized light. (E) Pure neovolcanic matrix-rich arenite; southern petrofacies, crossed nicols. (F) Vitric tuff. Glass shards shown by red arrows; southern petrofacies, polarized light.

Ternary compositional diagrams by themselves discriminate the arenite petrofacies of the southern Thrace Basin only partially. Integration of the most significant gross compositional parameters with heavy-mineral and paleocurrent data isolate two petrofacies cropping out in specific portions of the southern Thrace Basin: a southern and a northern petrofacies (south and north of the Ganos Fault, respectively). The southern petrofacies includes sandstone samples taken from the Gökçeada, Tayfur, and Şarköy stratigraphic sections; the northern petrofacies those taken from the Alexandroupolis, Korudağ, and Ganos Mt. stratigraphic sections

(Fig. 2). The petrographic characteristics of the two petrofacies and their distribution in the studied stratigraphic sections are illustrated in Figs. 2, 4, and 5. Their main petrographic, stratigraphic, and sedimentological features are described below in more detail.

### 6.1. Southern petrofacies

The southern petrofacies shows a distinctive vertical compositional and sedimentological evolution. The oldest stratigraphic interval south

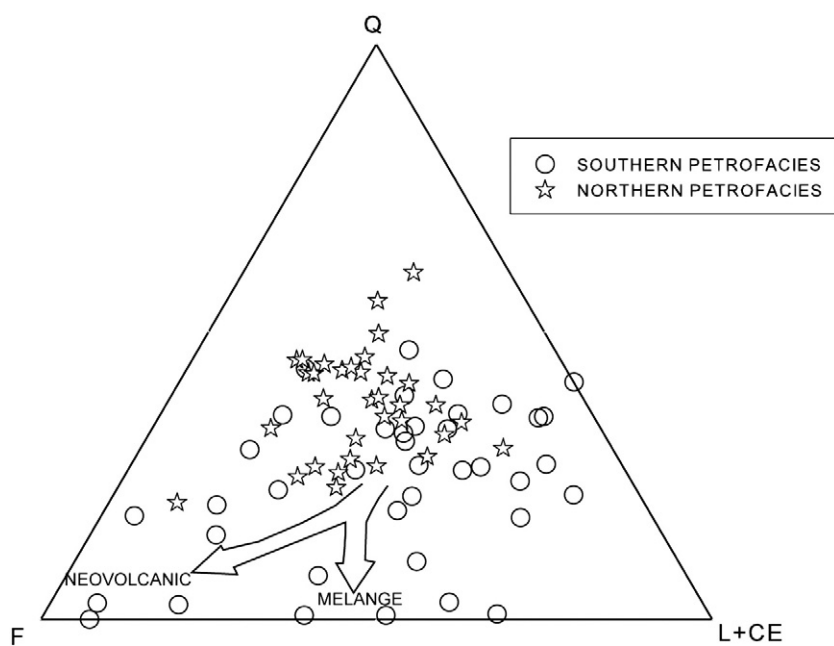


**Fig. 4.** Ternary compositional diagrams for sandstone petrofacies characterization. (A) Q, total quartz grains; F, total feldspar grains; L + CE, total aphanitic lithic fragments.

of the Ganos Fault (i.e. the Lower Eocene of the Tayfur stratigraphic section; Fig. 2) is characterized by arkosic litharenites and subordinate lithic arkoses with abundant epimetamorphic rock fragments associated with a significant amount of ophiolitic and terrigenous carbonate detritus (Fig. 4). Picotite is the only distinctive heavy mineral, in agreement with the presence of ophiolitic rock fragments. Paleocurrent indicators show NNE-ward flow, suggesting a source area located to the south of the basin.

The Middle Eocene section is characterized by litharenites dominated by low-grade metamorphic rock fragments. Ophiolitic rocks and picotite occur as in the Early Eocene section, but terrigenous carbonate grains are virtually absent. Traces of epidote and titanite are sporadically present. Average paleocurrent flow direction is toward the ESE. This petrofacies comprises the mid-Eocene fluvio-deltaic deposits and slope turbidites of the Gökçeada and Tayfur stratigraphic sections (Fig. 2). The mid-Eocene section differs from the Early Eocene one because of (i) its lower content of terrigenous carbonate and (ii) the eastward average paleoflow direction. The latter might indicate provenance from either the eastern Rhodopes–northern Aegean region or the southern basin margin, as a result of eastward deflection in the basin plain of a northward sediment dispersal pattern (Fig. 5).

The Upper Eocene–Early Oligocene south of the Ganos Fault is characterized by very immature arkose (Q content < 6%) and arkosic litharenite. This interval features abundant neovolcanic and intrabasinal carbonate grains (some samples are hybrid arenites, sensu Zuffa, 1980). Other common framework components are (i) epimetamorphic and ophiolitic rock fragments and (ii) glaucophane and picotite grains,

but their amounts are significantly lower compared to those of the Early–Middle Eocene section because the abundant carbonate intrabasinal and neo-volcanic grains dilute all other detrital components. Titanite and augite characterize further this petrostratigraphic interval. In the upper part of the Tayfur section (Fig. 2) the volcanic component is very abundant and slumped turbidite slope deposits, including a large olistolith of penecontemporaneous vitric tuff, indicate a north-facing paleoslope. Despite the fact that significant neovolcanic detritus is present only in the upper parts of the Tayfur and Şarköy sections, it should be noted that volcanic detritus – mostly penecontemporaneous – are somewhat present in the uppermost Eocene–Oligocene section throughout the study area. Overall detrital modes and the presence in several samples of glaucophane and epidote suggest a provenance from an exhumed subduction–accretion prism affected by volcanism.

6.2. Northern petrofacies

Sandstone samples north of the Ganos segment of the North Anatolian Fault have a well defined composition straddling the field between arkosic litharenite and lithic arkose (Fig. 4) and generally show a higher compositional maturity compared to those of the southern petrofacies. The Upper Eocene–Lower Oligocene Korudağ and Ganos Mountain stratigraphic sections are characterized by the presence of epidote and titanite. Paleocurrents indicate ENE-directed flow directions that may be compatible with eastward deflection of flows generated along the southern basin margin. Turbidite flows from the eastern Rhodopian area cannot be ruled out.

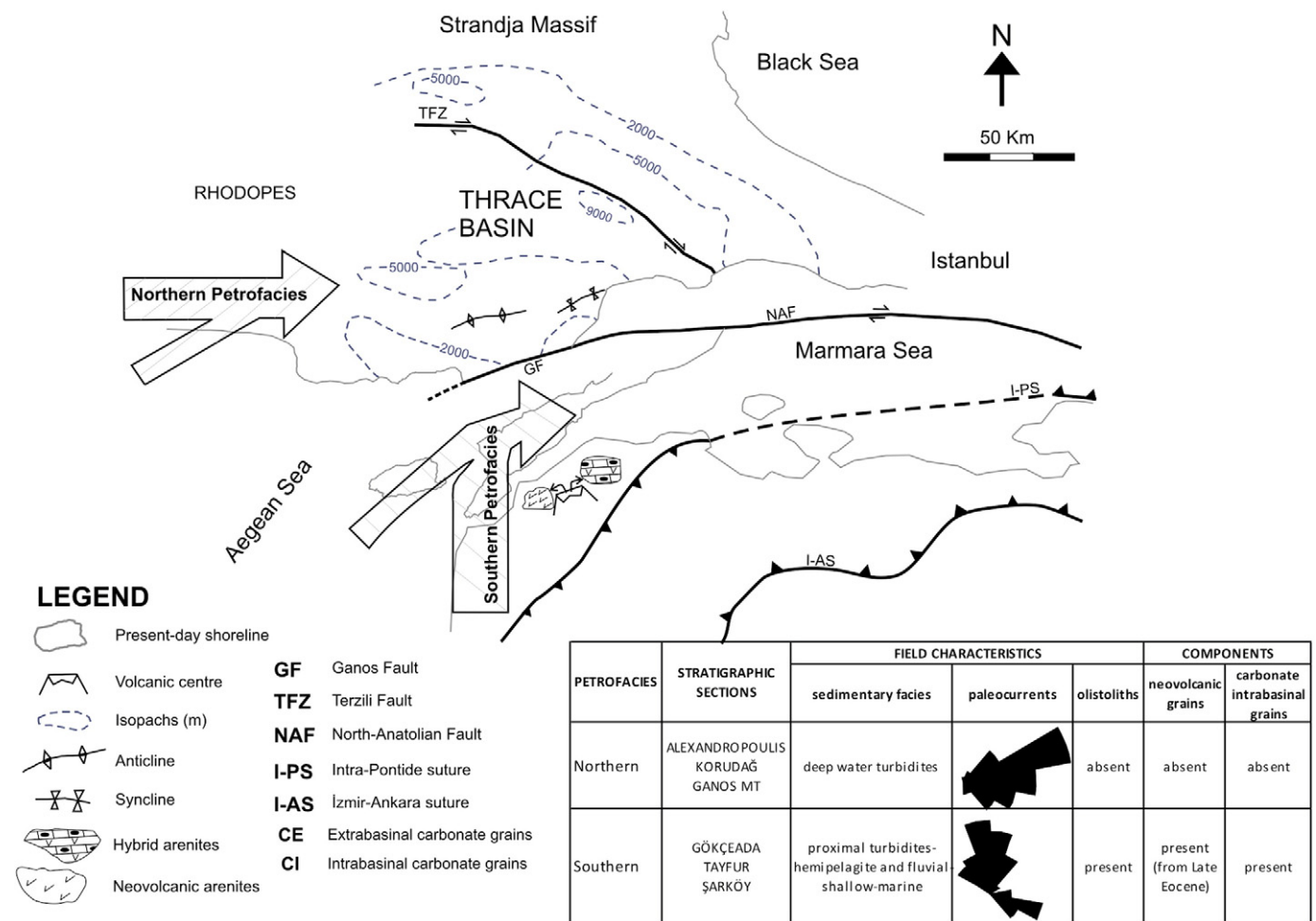


Fig. 5. Provenance and sand dispersal pattern (arrows) in the southern Thrace Basin. Inset at lower right summarizes main petrological and sedimentological features of northern and southern petrofacies. Plio-Quaternary dextral offset of about 60 km along the North Anatolian Fault was restored.

The Middle–Upper Eocene Alexandroupolis stratigraphic section is composed of litharenitic arkose. The amount of K-feldspar is characteristically higher than that of plagioclase. This section is characterized by (i) the abundance of coarse-grained granitoid/gneissic and fine-grained metamorphic lithic fragments, and (ii) the absence (or small amount) of ophiolitic and extrabasinal carbonate grains. The heavy mineral association is very simple, being represented by zircon, tourmaline, rutile, and garnet. Provenance was directly from the Rhodopian basement nearby. Paleocurrent measurements indicate ESE-directed paleoflows.

## 7. Discussion

The study area covers a significant portion of the Thrace Basin and the results of this study provide new compelling constraints on its sediment dispersal pattern and stratigraphic architecture. Fig. 5 is a tentative reconstruction of the Eocene sediment dispersal pattern of the southern Thrace Basin. In the figure, considering that our study area straddles the most active strand of the North Anatolian Fault system (Fig. 1), a conservative Plio-Quaternary dextral strike-slip offset of ca. 70 km (Armijo et al., 1999) was restored.

Zattin et al. (2005, 2010) showed that the Ganos segment of the North Anatolian Fault had a Late Oligocene precursor with a significant dip-slip component. Abrupt paleoenvironmental variations between time-equivalent stratigraphic horizons across the Ganos Fault seem to substantiate the notion that during the Eocene a structural discontinuity was already active along the trace of the present-day Ganos Fault, in line with the documented existence of a number of elongated structural highs and lows influencing the sediment dispersal pattern and the areal distribution of paleoenvironments across the Thrace Basin (e.g. Doust and Arikani, 1974; Perinçek, 1991; Turgut et al., 1991). Petrological, stratigraphic, and sedimentological data gathered during this study also point to a substantial compartmentalization of the sediment dispersal pattern of the southern Thrace Basin during the Eocene and the Early Oligocene. For this reason, we will discuss separately the characteristics of the stratigraphic sections located north and south of the Ganos segment of the North Anatolian Fault.

### 7.1. Successions located south of the Ganos Fault

Our petrographic analyses indicate that the provenance of the Lower Eocene Karaağaç turbidites (the oldest section in the study area) is predominantly from ophiolitic source rocks and their pelagic sedimentary cover. The Biga subduction/accretion wedge (Çetmi mélangé) – whether or not associated with the westward continuation of the Intra-Pontide suture – and the more southern İzmir–Ankara subduction/accretion wedge associated with the closure of a branch of the Neotethys (Okay and Tüysüz, 1999; Okay et al., 2001, 2008) are the obvious source-area candidates for the detritus forming this turbidite unit. A southern provenance is also shown by paleocurrent trends and paleoslope orientation as shown by slump features and olistoliths.

The samples from the red beds of the Fiçitepe Fm (Tayfur section) and the entire Gökçeada section come from a variety of sedimentary environments, from continental to deep marine. Despite a lower content in terrigenous carbonates, these samples have a composition very similar to those from the Karaağaç turbidites. Conversely, paleocurrent data indicate general sediment transport towards the east, in disagreement with the northward paleocurrents typical of the Karaağaç Fm. Time-equivalent deposits cropping out in northeastern mainland Greece and on Limnos Island were derived from the erosion of the Circum–Rhodopian Belt (Critelli et al., 2004; Marchev et al., 2004; Caracciolo, 2009). Therefore supply could be thought as the same for both the Greek and Turkish sectors of the Thrace Basin. However, if we compare the gross composition of the studied samples with those of the successions in the southeastern Rhodopes studied by Caracciolo (2009) they are substantially different. For this reason,

the hypothesis of a Rhodopian provenance of the mid-Eocene section south of the Ganos Fault can be excluded. Such sediments were instead most likely derived from the south and southwest, i.e. from the exhumed accretionary wedges mentioned above. Sediment paleodispersal of this deep-marine facies was then deflected toward the east along the axes of a number of elongated depocenters (Doust and Arikani, 1974; Perinçek, 1991; Turgut et al., 1991).

Pure neovolcanic fallout beds and turbidite strata of hybrid arenites compositionally characterize the Late Eocene–Early Oligocene of the Tayfur and Şarköy stratigraphic sections. The composition of the arenite framework, made of carbonate intrabasinal grains (bioclasts and peloids) and by pristine neovolcanic grains locally coated by carbonate rims (Fig. 3B), points to the existence of a shallow-water intrabasinal source area where carbonate grains were generated and mixed with pyroclastic detritus from penecontemporaneous volcanism. Such shallow-water sediment accumulations were then periodically mobilized as gravity flows and redeposited into slope/basinal environments, resulting in hybrid arenitic turbidites. As for the lower part of the southern petrofacies, granitic/gneissic, epimetamorphic and ophiolitic lithic grains, and picotite are present, but their amount is significantly lower because of the abundant carbonate intrabasinal grain and neo-volcanic grains that dilute all other components. Measurement of slump-fold axes around a large tuff olistolith in the Oligocene portion of the Tayfur Formation at the Tayfur dam (Section 2; Fig. 2) indicates deposition along a north-facing paleoslope.

The turbiditic succession of the Çengelli Formation (Okay et al., 2010) along the Şarköy stratigraphic section (Fig. 2) features thick proximal olistostromes and giant olistoliths. Clast composition is scale-invariant, from sand grains to olistoliths up to 1 km across: serpentinite, gabbro, basalt, greenschist, greywacke, Cretaceous–Paleocene pelagic limestone, and the underlying Upper Bartonian–Lower Priabonian Soğucak Limestone. Composite olistoliths consisting of pelagic limestone or basalt overlain by the Soğucak Limestone are common, providing further evidence of intense synsedimentary tectonics. The Upper Eocene mass flows of the Çengelli Fm were probably formed in an extensional setting and were derived from the south from the flanks of large normal or transtensional faults related to the opening of the southern Thrace Basin (Okay et al., 2010). The entire Şarköy section indicates a provenance from the ophiolitic suite of an exhumed subduction-accretion prism located to the south. The occurrence of glaucophane – even if in very small amounts – among the heavy-mineral association is in agreement with this interpretation. The Şarköy section also contains a significant amount of neovolcanic detritus and intrabasinal carbonate grains indicating a paleogeographic setting of the source/basin system somewhat analogous to the one described for the upper portion of the Tayfur section.

### 7.2. Successions located north of the Ganos Fault

The Alexandroupolis stratigraphic section has a provenance from upper crustal epimetamorphic rocks and a granitic–gneissic basement complex. Such provenance is coherent with the composition of the Rhodopian massif (Circum–Rhodopian Belt and Gneissic–Migmatitic Complex, Marchev et al., 2004). Our rather limited sandstone gross compositional data from Alexandroupolis are similar with those of the extensive dataset by Caracciolo (2009) and Caracciolo et al. (2007a, 2007b, 2011). Derivation of the detritus from the Rhodopian massif is also shown by (i) the mid-Eocene proximal, coarse-grained sedimentary facies (fan-deltas and alluvial fans) draining directly the basement terrains of the massif and (ii) consistent paleocurrents toward the ESE. It should be remarked that the middle Eocene part of this succession consists of a fluvial to shallow-marine sandstone and conglomerate; as a consequence, the provenance signal could have a strong local connotation. Despite this potential limitation, mid-Eocene sandstones across the Rhodopes have similar composition (Caracciolo, 2009).

The Korudağ and Ganos Mountain stratigraphic sections cover together the Middle Eocene–Late Oligocene time span and are both made of deep-sea turbidites gradually evolving upsection into slope, shelfal, and deltaic deposits (Fig. 2). Paleocurrent measurements from the study area north of the Ganos Fault indicate paleoflows consistently directed toward the ESE (see also Sümengen and Terlemez, 1991; Görür and Okay, 1996; Turgut and Eseller, 2000; Siyako and Huvaz, 2007). Such paleocurrents may be compatible with turbidite flows from either (i) the Rhodopian massif or (ii) the eastward deflection of turbidite flows originally derived from the southern basin margin. The fact that this petrofacies does not match a Rhodopian provenance (cf. Caracciolo, 2009) points to a southern provenance. In spite of being almost devoid of neovolcanic detritus, most sandstone samples from the Korudağ and Ganos Mt. sections are coeval with the neovolcanic-rich Upper Eocene–Oligocene turbidites of the Tayfur section (Fig. 2) for which we propose a source area characterized by an exhumed subduction/accretionary wedge with active volcanic centers. Volcaniclastic beds were observed locally in the northern limb of the Korudağ anticline but significant amounts of neovolcanic grains mixed with other siliciclastic detritus were not found in the analyzed samples. Therefore the sediment source areas for the southern part of the Thrace Basin north of the Ganos Fault during Eo-Oligocene times was most likely located to the south but the Tayfur succession does not seem to correspond to the main entry point for the turbidite currents that filled this portion of the Thrace basin.

In summary, the integration of (i) gross composition modal analyses, (ii) heavy-mineral analyses, (iii) paleocurrent analysis, and (iv) qualitative sedimentological observations indicates that the southern part of the Thrace Basin was fed by ophiolitic detritus *latu sensu* coming from the south, i.e. from the İzmir–Ankara and Biga (Intra-Pontide?) subduction/accretion complexes. The Thrace Basin developed during the complex transition between the collisional tectonic regime following the closure of the Vardar–İzmir–Ankara oceanic realm and the extensional regime characterizing the Neogene evolution of the Aegean and periAegean regions. It was long interpreted as a forearc basin which developed in a context of northward subduction (Görür and Okay, 1996). This interpretation is challenged by this study and by Caracciolo (2009), both showing that penecontemporaneous volcanism kicked off late in the basin evolution (Innocenti et al., 1984; Yanev, 1998; Yanev et al., 1998), in contrast with typical forearc basins (for a review, see Dickinson, 1995). Besides, a belt of chaotic deposits in the Şarköy region, formerly interpreted as a tectonic *mélange* formed in an accretionary prism delimiting the basin to the south (Beccaletto, 2004; Beccaletto et al., 2005), was recently mapped by Okay et al. (2010) as an Eocene olistostromal succession. Although there are several examples of sedimentary reworking of tectonic *mélange* from accretionary prisms into adjacent forearc basins (see Cavazza and Barone, 2010, for a review), the long time span (>30 Ma) between the youngest age of the Çetmi *mélange* (Turonian) and the base of the Thrace basin fill indicates that the accretionary prism was inactive when the Thrace Basin was formed. The Thrace Basin may instead be the result of either (i) post-orogenic collapse after the continental collision related to the closure of the Vardar Ocean, or (ii) upper-plate extension related to slab retreat in front of the Pindos remnant ocean.

The Rhodope Massif may represent a significant sediment source rock area for the central and northern portions of the basin fill but our study, being focused on the southern portion of the basin, does not provide conclusive constraints on this issue.

## 8. Conclusions

This study underscores how the detailed temporal and spatial interpretation of the provenance of volcanic and carbonate clastic particles, coupled with more traditional stratigraphic/sedimentologic techniques, is crucial (i) for correct paleogeographic/paleoenvironmental

reconstructions and (ii) for the determination of the geodynamic setting of ancient sedimentary basins. Sandstone petrologic data and the synthesis of preexisting and new sedimentologic observations along representative stratigraphic sections in the southern portion of the Thrace Basin show that an important sediment source area was located to the south, along the İzmir–Ankara suture and the Biga suture. Sediment derived from the erosion of the orogenic prism is characterized by ophiolitic detritus, including a deep-sea sedimentary cover. Epimetamorphic and granitoid detritus is also present. Starting from Late Eocene time, a significant penecontemporaneous volcanic component is also present. The coexistence of pure neovolcanic layers (crystal tuffs) and hybrid carbonate-rich arenites with detritus derived from a continental basement indicates the presence of episutural basins where shallow-water carbonates were deposited on top of the exhuming subduction–accretion prism. These carbonates were mixed with penecontemporaneous neovolcanic components and redeposited in deeper marine environments. The entire southern Thrace Basin was fed from the south and southwest, as shown by this distinctively abundant ophiolitic detrital input which is very minor or altogether absent along the other basin margins.

Other elements pointing to a southern provenance are (i) large olistoliths and olistostromes recently mapped interbedded in the Eocene turbidites in the Şarköy region along the southern margin of the basin (Okay et al., 2010), and (ii) large Oligocene deltaic bodies generically prograding northeastward in the same region (Osmançik Formation, Atalik, 1992). Both elements point to a protracted history of northward sediment dispersal, in agreement with our sandstone petrographic data and sedimentological observations. Only the most proximal facies show northward paleocurrents whereas most measured paleocurrent indicators show an eastward paleoflow, most likely the result of gravity flow deflection. During most of the Eocene the entire basin was characterized by a complex physiography, as shown by both commercial seismic lines (e.g. Turgut et al., 1991) and dramatic lateral facies changes at the surface (e.g. Siyako and Huvaz, 2007). Such configuration was controlled by generically east–west trending transtensional fault systems that influenced sediment dispersal and the areal distribution of paleoenvironments.

A second sediment source area was the plutono-metamorphic Rhodope Massif west of the basin. The detritus generated in this area was then dispersed eastward and likely filled the northern and central sectors of the Thrace Basin. The coarse-grained fan–deltas characterizing the Eocene section along the western margin of the basin in Greece and Bulgaria were the entry points associated with this second sediment source area (Caracciolo et al., 2007a, b, 2011; Caracciolo, 2009).

## Acknowledgments

Reviews by Luca Caracciolo and an anonymous reviewer are gratefully acknowledged. Luis Arribas provided insights on the diagenetic interpretation. An earlier draft of the manuscript was reviewed by Gert Jan Weltje. This research was sponsored by MIUR (Italian Dept. of Public Education, University and Research) and by TÜBA (The Turkish Academy of Sciences). Field assistance by Zeynep Erdem is gratefully acknowledged.

## Appendix A. Supplementary data

Supplementary data to this article can be found online at doi:10.1016/j.sedg.2011.10.008

## References

- Aksoy, Z., 1987. Depositional environment of the sequences in the Barbaros–Keşan–Kadıköy–Gaziköy region (southern Thrace). Proceedings of the 7th Petroleum Congress of Turkey, Ankara, pp. 292–311 (in Turkish).
- Armijo, R., Meyer, B., Hubert, A., Barka, A., 1999. Westward propagation of the North Anatolian fault into the northern Aegean: timing and kinematics. *Geology* 27, 267–270.

- Atalik, E., 1992. Depositional systems of the Osmancik Formation in the Thrace basin. PhD dissertation, Middle East Technical University, 366 pp.
- Beccaletto, L., 2004. Geology, correlations and geodynamic evolution of the Biga Peninsula (NW Turkey). PhD dissertation, Université de Lausanne, Suisse.
- Beccaletto, L., Bartolini, A.C., Martini, R., Hochuli, P.A., Kozur, H., 2005. Biostratigraphic data from the Çetmi Melange, northwest Turkey: palaeogeographic and tectonic implications. *Palaeogeography, Palaeoclimatology, Palaeoecology* 221, 215–244.
- Bonev, N., 2006. Cenozoic tectonic evolution of the Eastern Rhodope Massif (Bulgaria): basement structure and kinematics of syn to postcollisional extensional deformation. Geological Society of America Special Paper, pp. 211–235.
- Bonev, N., Beccaletto, L., 2007. From syn- to post-orogenic Tertiary extension in the north Aegean region: constraints on the kinematics in the eastern Rhodope–Thrace, Bulgaria–Greece and the Biga Peninsula, NW Turkey. Geological Society, London, Special Publications, 291, pp. 113–142.
- Burchfiel, B.C., Nakov, R., Tzankov, T., Royden, L.H., 2000. Cenozoic extension in Bulgaria and northern Greece: the northern part of the Aegean extensional regime. In: Bozkurt, E., Winchester, J.A., Piper, J.D.A. (Eds.), *Tectonics and Magmatism in Turkey and the Surrounding Area*, 173. Geological Society of London, Special Publications, pp. 325–352.
- Burg, J.-P., Ricou, L.-E., Ivanov, Z., Godfriaux, J., Dimov, D., Klain, L., 1996. Syn-metamorphic nappe complex in the Rhodope Massif, structure and kinematics. *Terra Nova* 8, 6–15.
- Caracciolo, L., 2009. The interplay of accretionary processes and magmatic arcs in forming stratigraphic sequences in the Circum-Rhodope Belt, Greece and Bulgaria. PhD dissertation, University of Calabria, Italy, 150 pp.
- Caracciolo, L., Critelli, S., Innocenti, F., Kolios, N., Manetti, P., von Eynatten, H., 2007a. Significance of Geochemical Signatures on Provenance in Eocene Sandstone Sequences, Rhodopian Orogen. *Int. Ass. Sedimentologists Reg. Meet., Patraso, Greece*. (Abstract Book).
- Caracciolo, L., Critelli, S., Innocenti, F., Kolios, N., Manetti, P., 2007b. Composition and Provenance of the Eocene–Miocene Sandstones of the Rhodopian Orogen. *Int. Ass. Sedimentologists Reg. Meet., Patraso, Greece*. (Abstract Book).
- Caracciolo, L., Critelli, S., Innocenti, F., Kolios, N., Manetti, P., 2011. Unravelling provenance from Eocene–Miocene sandstones of the Thrace Basin, NE Greece. *Sedimentology* 58, 1988–2011.
- Cavazza, W., Barone, M., 2010. Large-scale sedimentary recycling of tectonic mélange in a forearc setting: the Ionian basin (Oligocene–Quaternary, southern Italy). *Geological Society of America Bulletin* 122, 1932–1949.
- Cavazza, W., Okay, A.I., Zattin, M., 2009. Rapid early–middle Miocene exhumation of the Kazdağ metamorphic core complex (Western Anatolia). *International Journal of Earth Sciences* 98, 1935–1947. doi:10.1007/s00531-008-0353-9.
- Chayes, F., 1952. Notes of the staining of potash feldspar with sodium cobaltinitrite in thin section. *American Mineralogist* 37, 337–340.
- Cibin, U., Di Giulio, A., 1996. Proposta di normativa per l'analisi microscopica della composizione delle areniti nell'ambito della Carta Geologica d'Italia a scala 1:50.000. *Bollettino del Servizio Geologico d'Italia* 115, 87–98.
- Critelli, S., Ingersoll, R.V., 1995. Interpretation of neovolcanic versus palaeovolcanic sand grains – an example from Miocene deep-marine sandstones of the Topanga Group (southern California). *Sedimentology* 42, 783–804.
- Critelli, S., Innocenti, F., Manetti, P., 2004. Unravelling magmatic and orogenic provenance for the Eocene to Miocene sandstone detrital modes of the island of Limnos, Hellenic arc, Greece. (Abstract) 32nd International Geological Congress. (Florence).
- Crook, K.A.W., 1974. Lithogenesis and geotectonics: the significance of compositional variations in flysch arenites (graywackes). In: Dott, R.H., Shaver, R.H. (Eds.), *Modern and Ancient Geosynclinal Sedimentation*. SEPM Special Publication, 19, pp. 304–310.
- d'Atri, A., 2010. Provenienza dei sedimenti arenitici nel Bacino di Tracia (Eo-Oligocene, Turchia nord-occidentale e Grecia nord-orientale). PhD dissertation, University of Bologna, 115 pp. [http://amsdottorato.cib.unibo.it/2667/1/d'atri\_azzurra\_tesi.pdf]
- De Rosa, R., Zuffa, G.G., Taira, A., Leggett, J.K., 1986. Petrography of trench sands from the Nankai Trough, southwest Japan: implications for long-distance transportation. *Geological Magazine* 123, 477–486.
- Di Vincenzo, G., Viti, C., Rocchi, R., 2003. The effect of chlorite interlayering on  $^{40}\text{Ar}$ – $^{39}\text{Ar}$  biotite dating: an  $^{40}\text{Ar}$ – $^{39}\text{Ar}$  laserprobe and TEM investigation of variably chloritised biotites. *Contributions to Mineralogy and Petrology* 145, 643–658.
- Di Vincenzo, G., Bracciali, L., Del Carlo, P., Panter, K., Rocchi, S., 2010.  $^{40}\text{Ar}$ – $^{39}\text{Ar}$  dating of volcanogenic products from the AND-2A core (ANDRILL Southern McMurdo Sound Project, Antarctica): correlations with the Erebus Volcanic Province and implications for the age model of the core. *Bulletin of Volcanology* 72, 487–505.
- Dickinson, W.R., 1970. Interpreting detrital modes of graywacke and arkose. *Journal of Sedimentary Petrology* 40, 695–707.
- Dickinson, W.R., 1985. Interpreting provenance relations from detrital modes of sandstone. In: Zuffa, G.G. (Ed.), *Provenance of Arenites*. Kluwer Academic Publishers, pp. 333–361.
- Dickinson, W.R., 1995. Forearc basins. In: Busby, C.J., Ingersoll, R.V. (Eds.), *Tectonics of Sedimentary Basins*. Blackwell Science, Oxford, pp. 221–262.
- Dickinson, W.R., Suczek, C.A., 1979. Plate tectonics and sandstone composition. *American Association of Petroleum Geologists Bulletin* 63, 2164–2182.
- Dickinson, W.R., Beard, L.S., Brakenridge, C.R., Erjavec, J.L., Ferguson, R.C., Inman, K.F., Knepp, R.A., Lindberg, F.A., Ryberg, P.T., 1983. Provenance of North America Phanerozoic sandstones in relation to tectonic setting. *Geological Society of America Bulletin* 94, 222–235.
- Doust, H., Arıkan, Y., 1974. The geology of the Thrace basin. *Proceedings of the 7th Petroleum Congress of Turkey*, Ankara, pp. 119–136.
- Fontana, D., Zuffa, G.G., Garzanti, E., 1989. The interaction of eustasy and tectonism from provenance studies of the Eocene Hecho Group Turbidites (South-Central Pyrenees, Spain). *Basin Research* 2, 223–237.
- Gandolfi, G., Paganelli, L., Zuffa, G.G., 1983. Petrology and dispersal pattern in the Marnoso-Arenacea Formation (Miocene, northern Apennines). *Journal of Sedimentary Petrology* 53, 493–507.
- Gandolfi, G., Paganelli, L., Cavazza, W., 2007. Heavy-mineral associations as tracers of limited compositional mixing during turbiditic sedimentation of the Marnoso-arenacea Formation (Miocene, Northern Apennines, Italy). In: Mange, M.A., Wright, D.T. (Eds.), *Heavy Minerals in Use. : Developments in Sedimentology*, 58. Elsevier, pp. 681–706.
- Garzanti, E., Dogliani, C., Vezzoli, G., Andò, S., 2007. Orogenic belts and sediment provenance. *Journal of Geology* 115, 315–334.
- Gazzi, P., 1966. Le arenarie del flysch sopracretaceo dell'Appennino modenese; correlazioni con il flysch di Monghidoro. *Mineralogica et Petrographica Acta* 12, 69–97.
- Gazzi, P., Zuffa, G.G., Gandolfi, G., Paganelli, L., 1973. Provenienza e dispersione litoranea delle sabbie delle spiagge adriatiche fra le foci dell'Isonzo e del Foglia: inquadramento regionale. *Memorie Società Geologica Italiana* 12, 1–37.
- Görür, N., Okay, A.I., 1996. A fore-arc origin for the Thrace Basin, NW Turkey. *Geologische Rundschau* 85, 662–668.
- Görür, N., Monod, O., Okay, A.I., et al., 1997. Palaeogeographic and tectonic position of the Carboniferous rocks of the western Pontides (Turkey) in the frame of the Variscan belt. *Bull. Soc. Geol. France* 168, 197–205.
- Gradstein, F.M., Ogg, J.G., Smith, A.G., et al., 2004. *A Geological Time Scale 2004*. Cambridge University Press.
- Hathway, B., Kelley, S.P., 2000. Sedimentary record of explosive silicic volcanism in a Cretaceous deep-marine conglomerate succession, northern Antarctic Peninsula. *Sedimentology* 47, 451–470.
- Ingersoll, R.V., Suczek, C.A., 1979. Petrology and provenance of Neogene sand from Nicobar and Bengal fans, DSDP sites 211 and 218. *Journal of Sedimentary Petrology* 49, 1217–1228.
- Ingersoll, R.V., Bullard, T.F., Ford, R.L., Grimm, J.B., Pickle, J.D., Sares, S.W., 1984. The effect of grain size on detrital modes: a test of the Gazzi–Dickinson point-counting method. *Journal of Sedimentary Petrology* 54, 103–116 (Also, see discussions and replies: 55, 616–621.).
- Ingersoll, R.V., Cavazza, W., Graham, S.A., Participants, Indiana Geologic Field Seminar, 1987. Provenance of impure calcilithites in the Laramide foreland of southwestern Montana. *Journal of Sedimentary Petrology* 57, 995–1003.
- Innocenti, F., Kolios, N., Manetti, P., Mazzuoli, R., Peccerillo, A., Rita, F., Villari, L., 1984. Evolution and geodynamic significance of the Tertiary orogenic volcanism in Northeastern Greece. *Bulletin Volcanologique* 47, 25–37.
- Johnsson, M.J., Basu, A., 1993. Processes controlling the composition of clastic sediments. *Geological Society of America Special Paper*, 284. (342 p.).
- Kellog, H.E., 1973. Geology and petroleum prospects of the Gulf of Saros and vicinity (southwestern Thrace). TPAO Report 902. Ashland Oil of Turkey Inc, Ankara.
- Keskin, E., 1984. Pınarhisar alaninin jeolojisi. *Türkiye Jeoloji Kurumu Bülteni* 14, 31–84.
- Krohe, A., Mposkos, A., 2002. Multiple generations of extensional detachments in the Rhodope Mountains (northern Greece): evidence of episodic exhumation of high-pressure rocks. *Geol. Soc. London Spec. Publ.*, 204, pp. 151–178.
- Lindholm, R.C., Finkelman, R.B., 1972. Calcite staining: semi-quantitative determination of ferrous iron. *Journal of Sedimentary Petrology* 42, 239–245.
- Mack, G.H., 1984. Exceptions to the relationship between plate tectonics and sandstone composition. *Journal of Sedimentary Petrology* 54, 212–220.
- Maratos, G., Andronopoulos, V., Koukouzas, K., 1977. *Geological Map of Greece*. Alexandroupolis Sheet, scale 1:50,000. IGME, Athens.
- Marchev, P., Raicheva, R., Downes, H., Vaselli, O., Chiaradia, M., Moritz, R., 2004. Compositional diversity of Eocene–Oligocene basaltic magmatism in the Eastern Rhodopes, SE Bulgaria: implications for genesis and tectonic setting. *Tectonophysics* 393, 301–328.
- Morton, A.C., Halls, C.R., 1999. Processes controlling the composition of heavy mineral assemblages in sandstones. *Sedimentary Geology* 124, 3–29.
- Okay, A.I., Tüysüz, O., 1999. Tethyan sutures of northern Turkey. In: Durand, B., Jolivet, L., Horvath, F., Seranne, M. (Eds.), *The Mediterranean Basins: Tertiary Extension within the Alpine Orogen*. Geological Society of London, Special Publications, 156, pp. 475–515.
- Okay, A.I., Siyako, M., Bürkan, K.A., 1991. Geology and tectonic evolution of the Biga peninsula, northwest Turkey. *Bull. Tech. Univ. Istanbul* 44, 191–256.
- Okay, A.I., Satir, M., Tüysüz, O., Akyüz, S., Chen, F., 2001. The tectonics of the Strandja Massif: late-Variscan and mid-Mesozoic deformation and metamorphism in the northern Aegean. *International Journal of Earth Sciences* 90, 217–233.
- Okay, A.I., Tuysuz, O., Kaya, S., 2004. From transpression to tension: changes in morphology and structure around a bend on the North Anatolian Fault in the Marmara region. *Tectonophysics* 391, 259–282.
- Okay, A.I., Satir, M., Zattin, M., Cavazza, W., Topuz, G., 2008. An Oligocene ductile strike-slip shear zone: the Uludağ Massif, northwest Turkey – implication for the westward translation of Anatolia. *Geological Society of America Bulletin* 120, 893–911.
- Okay, A.I., Özcan, E., Cavazza, W., Okay, N., Less, G., 2010. Basement types, Lower Eocene series, Upper Eocene olistostromes and the initiation of the southern Thrace Basin, NW Turkey. *Turkish Journal of Earth Sciences* 19, 1–25. doi:10.3906/yer-0902-10.
- Okay, N., Zack, T., Okay, A.I., Barth, M., 2011. Sinistral transport along the Trans-European Suture Zone: detrital zircon-rutile geochronology and sandstone petrography from the Carboniferous flysch of the Pontides. *Geological Magazine* 148, 380–403.
- Önal, M., 1986. Sedimentary facies and tectonic evolution of the central part of the Gelibolu Peninsula, NW Anatolia, Turkey. *Jeoloji Mühendisliği* 29, 37–46 (in Turkish).
- Özcan, E., Less, G., Okay, A.I., Baldi-Beke, M., Kollányi, K., Yilmaz, I.Ö., 2010. Stratigraphy and larger foraminifera of the Eocene shallow-marine and olistostromal units of the southern part of the Thrace Basin, NW Turkey. *Turkish Journal of Earth Sciences* 19, 27–77.
- Özgürüş, Z., Okay, A.I., Özcan, E., 2009. Late-Cretaceous–Eocene evolution of the western margin of the İstanbul and Sakarya zones. Abstracts, 62. Geological Congress of Turkey, Ankara, p. 462.
- Pal, T., Gupta, T.D., Chakraborty, P.P., Das Gupta, S.C., 2005. Pyroclastic deposits of Miocene age in the Arakan Yoma–Andaman–Java subduction complex, Andaman Islands, Bay of Bengal, India. *Geochemical Journal* 39, 69–82.

- Papadopoulos, P., 1980. Geological Map of Greece. Ferai sheet, scale 1:50,000. IGME, Athens.
- Perinçek, D., 1991. Possible strand of the North Anatolian fault in the Thrace Basin, Turkey – an interpretation. *American Association of Petroleum Geologists Bulletin* 75, 241–257.
- Şen, Ş., 2002. Collisional-backthrust basin model for the Thrace–Göynük–Safranbolu basin (NW Turkey). *International Conference on Earth Sciences and Electronics (ICESE-2002)*, pp. 65–76.
- Şengör, A.M.C., 1979. The North Anatolian transform fault: its age, offset and tectonic significance. *Journal of the Geological Society of London* 136, 269–282.
- Şengör, A.M.C., Yılmaz, Y., 1981. Tethyan evolution of Turkey: a plate tectonic approach. *Tectonophysics* 75, 181–241.
- Siyako, M., 2006. Tertiary rock units of the Thrace Basin. *Lithostratigraphic Units of the Thrace Region. : Litostratigrafi Birimleri Serisi, 2. Publication of the General Directorate of the Mineral Research and Exploration (MTA), Ankara*, pp. 43–83 (in Turkish).
- Siyako, M., Huvaz, O., 2007. Eocene stratigraphic evolution of the Thrace basin, Turkey. *Sedimentary Geology* 198, 75–91.
- Siyako, M., Bürkan, K.A., Okay, A.I., 1989. Tertiary geology and hydrocarbon potential of the Biga and Gelibolu peninsula. *TPJD Bülteni* 1/3, pp. 183–199 (in Turkish).
- Stampfli, G.M., Borel, G.D., 2004. The TRANSMED transects in space and time: constraints on the Paleotectonic evolution of the Mediterranean domain. In: Cavazza, W., Roure, F., Spakman, W., Stampfli, G.M., Ziegler, P. (Eds.), *The TRANSMED Atlas: The Mediterranean Region from Crust to Mantle*. Springer Verlag, pp. 53–80.
- Stampfli, G., Hochard, C., 2009. Plate tectonics of the Alpine realm. *Geological Society of London Special Publications* 327, 89–111.
- Sümengen, M., Terlemez, I., 1991. Stratigraphy of Eocene sediments in the southwest Thrace. *Mineral Res. Expl. Bull.* 113, 15–29.
- Sümengen, M., Terlemez, I., Şentürk, K., Karaköse, C., 1987. Stratigraphy, sedimentology and tectonics of the Gelibolu Peninsula and southwestern Thrace Basin. *Internal Report of the Maden Tetkik ve Arama Enstitüsü 8128, Ankara.* (in Turkish).
- Temel, R.Ö., Çiftçi, N.B., 2002. Stratigraphy and depositional environments of the Tertiary sedimentary units in the Gelibolu Peninsula and on the islands of Gökçeada and Bozcaada (northern Aegean region, Turkey). *TPJD Bülteni*, 14, pp. 17–40 (in Turkish).
- Turgut, S., Eseller, G., 2000. Sequence stratigraphy, tectonics and depositional history in eastern Thrace Basin, NW Turkey. *Marine and Petroleum Geology* 17, 61–100.
- Turgut, S., Türkaslan, M., Perinçek, D., 1991. Evolution of the Thrace sedimentary basin and its hydrocarbon prospectivity. In: Spencer, A.M. (Ed.), *Generation, Accumulation, and Production of Europe's Hydrocarbons*. Special Publication of European Association of Petroleum Geoscientists 1, 415–437.
- Tüysüz, O., Barka, A., Yiğitbaş, E., 1998. Geology of the Saros graben and its implications for the evolution of the North Anatolian fault in the Ganos–Saros region, north-western Turkey. *Tectonophysics* 293, 105–126.
- Valloni, R., 1985. Reading provenance from modern sands. In: Zuffa, G.G. (Ed.), *Provenance of Arenites*. Kluwer Academic Publishers, pp. 309–332.
- Valloni, R., Maynard, J.B., 1981. Detrital modes of recent deep-sea sands and their relation to tectonic setting: a first approximation. *Sedimentology* 28, 75–83.
- Valloni, R., Zuffa, G.G., 1984. Provenance changes for arenaceous formations of the northern Apennines, Italy. *Geological Society of America Bulletin* 95, 1035–1039.
- Varol, B., Sirel, E., Ayyıldız, T., Baykal, M., 2007. New sedimentological and paleontological data from the Soğucak Formation in the Bozcaada (Çanakkale). *Bulletin of the Mineral Research and Exploration Institute (MTA) of Turkey*, 135, pp. 83–86 (in Turkish).
- Weltje, G.J., 2006. Ternary sandstone composition and provenance: an evaluation of the Dickinson model. In: Buccianti, A., Mateu-Figueras, Pawlowsky-Glahn, V. (Eds.), *Compositional Data Analysis in the Geosciences: From Theory to Practice*. *Geol. Soc. London Spec. Publ.*, 264, pp. 79–99.
- Yaltırak, C., Alpar, B., 2002. Kinematics and evolution of the northern branch of the North Anatolian Fault (Ganos fault) between the Sea of Marmara and the Gulf of Saros. *Marine Geology* 190, 351–366.
- Yanev, Y., 1998. Petrology of the Eastern Rhodopes Paleogene acid volcanics, Bulgaria. *Acta Vulcanologica* 10, 279–291.
- Yanev, Y., Innocenti, F., Manetti, P., Serri, G., 1998. Upper Eocene Oligocene collision related volcanism in Eastern Rhodope (Bulgaria) Western Thrace (Greece): petrogenetic affinity and geodynamic significance. *Acta Vulcanologica* 10, 265–277.
- Yıldız, A., Toker, V., Şengüler, I., 1997. The nannoplankton biostratigraphy of the Middle Eocene–Oligocene units in southern Thrace basin and the surface water temperature variations. *Türkiye Petrol Jeologları Derneği Bülteni* 9, 31–44.
- Yılmaz, Y., Polat, A., 1998. Geology and evolution of the Thrace volcanism, Turkey. *Acta Vulcanologica* 10, 293–303.
- Zattin, M., Okay, A.I., Cavazza, W., 2005. Fission-track evidence for late Oligocene and mid-Miocene activity along the North Anatolian Fault in south-western Thrace. *Terra Nova* 17, 95–101. doi:10.1111/j.1365-3121.2004.00583.x.
- Zattin, M., Cavazza, W., Okay, A.I., Federici, I., Fellin, G., Pignalosa, A., Reiners, P., 2010. A precursor of the North Anatolian Fault in the Marmara Sea region. *Journal of Asian Earth Sciences* 39, 97–108. doi:10.1016/j.jseas.2010.02.014.
- Zuffa, G.G., 1980. Hybrid arenites: their composition and classification. *Journal of Sedimentary Petrology* 50, 21–29.
- Zuffa, G.G., 1985. Optical analyses of arenites: influence of methodology on compositional results. In: Zuffa, G.G. (Ed.), *Provenance of Arenites*. Kluwer Academic Publishers, pp. 165–189.
- Zuffa, G.G., 1987. Unravelling hinterland and offshore palaeogeography from deep-water arenites. *Marine Clastic Sedimentology* 39–61.
- Zuffa, G.G., 1991. On the use of turbidite arenites in provenance studies – critical remarks. In: Morton, A.C., Todd, S.P., Haughton, P.D.W. (Eds.), *Developments in Sedimentary Provenance Studies*. *Geol. Soc. London Spec. Publ.*, 57, pp. 21–28.